Electronic Supplementary Material (ESI) for Soft Matter.

Supporting Information: Quantitative diffusion and swelling kinetic measurements using large-angle interferometric refractometry

John E. Saunders, Hao Chen, Chris Brauer, McGregor Clayton, Weijian Jason Chen, Jack A. Barnes, and Hans-Peter Loock*

Department of Chemistry, Queen's University, Kingston, Ontario, K7L 3N6, Canada

* Email: hploock@queensu.ca

Section 1: Propagation of a light ray through a medium with a refractive index gradient

In the main paper an effective refractive index of the film, $\overline{n}_{film}$, in equation (2) is calculated from the interferometric phase, ϕ. We also use this effective refractive index in our model of the sorbate diffusion through the film (equation (24) in the main text). In the following paragraphs we test whether it is legitimate to approximate the refractive index gradient that is present in the non-equilibrated film with an average refractive index. We then estimate the error due to this necessary approximation.

We divide the film with thickness d and refractive index $n(y)$ into several layers, i, with thickness δy. The incidence angle into the bottom layer is governed by the refractive index contrast between the substrate and that layer:

$$\sin\left(\theta_0\right) = \sin\left(\theta_{substrate}\right)\frac{n_{substrate}}{n_0} \qquad \text{* MERGEFORMAT (S1)}$$

For each layer above this bottom layer, the angle is modified according to Snell's law:

$$\sin\left(\theta_{i+1}\right) = \sin\left(\theta_i\right)\frac{n_i}{n_{i+1}} \qquad \text{* MERGEFORMAT (S2)}$$

In each layer the ray travels a distance of

$$dL_i = \frac{dx}{\cos\left(\theta_i\right)} \qquad \text{* MERGEFORMAT (S3)}$$

and experiences an incremental phase shift of $n_i\, dL_i$. The total phase shift

$$\Delta\phi_{exact} = \sum_i n_i dL_i \qquad \text{* MERGEFORMAT (S4)}$$

is identical to the optical path. This optical path may be compared to that of the straight ray obtained from the average refractive index of all layers of the film

$$\Delta\phi_{ave} = n_{ave} L_{ave} \qquad \text{* MERGEFORMAT (S5)}$$

where

$$L_{ave} = \frac{d}{\sqrt{1 - \left(\frac{n_{substrate}}{n_{ave}} \sin\left(\theta_{substrate}\right) \right)^2}} \qquad \text{* MERGEFORMAT (S6)}$$

A simple calculation using a spreadsheet program shows that the difference between the exact phase delay $\Delta\phi_{exact}$ from equation * MERGEFORMAT (S4) and the approximate delay using an average value of the refractive index (equation * MERGEFORMAT (S5)) is more than about 1% only when the following conditions are met: the incidence angle θ_0 is within less than 0.2^0 of the critical angle and the refractive index gradient is larger than experimentally observed (n_{max} - $n_0 > 10^{-3}$).

Figures S1(A) and (B) show ray diagrams calculated using the above model. Here, the ray propagation is calculated at incidence angles that are 0.1^0 or 0.2^0 below the critical incidence angle of $\theta_c = 64.38^0$. In the calculation we used $n_0 = 1.572$, and $d = 40$ μm. We determined the optical pathlength, $\Delta\phi_{exact}$, of the curved ray using equation * MERGEFORMAT (S4) with 400 ray segments. The calculations were performed for 3 different refractive index gradients as shown in **Figure S1(C)**. Two of these gradients were defined to be a linear increase and a linear decrease of the index by $\Delta n = 10^{-3}$ over the height of the film; the third gradient is obtained using the model shown in Figure 4A of the main text with the experimentally obtained diffusion constant and at a time of 100s after the start of the experiment.

The optical pathlengths $\Delta\phi_{exact}$ were then compared to those obtained from the respective average refractive index value, $\Delta\phi_{ave}$ (eqn * MERGEFORMAT (S5)) with refractive indices - shown as dashed horizontal lines in **Figure S1(C)**. For $\theta_0 = \theta_c - 0.2^0 = 64.18^0$ the difference between $\Delta\phi_{exact}$ and $\Delta\phi_{ave}$ was 0.3% in the case of increasing refractive index and 0.7% in case of the decreasing refractive index. For $\theta_0 = \theta_c - 0.1^0 = 64.28^0$ the difference between $\Delta\phi_{exact}$ and $\Delta\phi_{ave}$ was 0.9% in the case of increasing refractive index and 5.4% in case of the decreasing refractive index. In the experiment the refractive index increases by at most 9×10^{-4} towards the surface as long as the system is not equilibrated. Using an estimate for the experimental index gradient the

difference in optical path is calculated to be even smaller, i.e. 0.26% at 0.2^0 below the critical angle and 0.84% at 0.1^0 below the critical angle.

While these deviations appear very small, we note that they do affect the position of those fringes associated with very high (glancing) incidence angles. Measurements of film thickness and refractive index can therefore not accurately be obtained if one uses *only* angles within 0.2^0 of the critical angle. If one assumes a constant thickness, the measured refractive index measurement could deviate by 2.6×10^{-3} from the exact average value – much more than might be expected from the analysis presented in the main paper!

We note that for films with a thickness around 40 μm the instrument does not record fringes from angles higher than θ_c - 0.2^0 and that rays at angles $\theta > \theta_c$ - 0.2^0 are much less affected by index gradients. It then appears justified to approximate the index gradients with an average index. This inability to create interference from these highest incidence angles is due to the large displacement of the exiting beam from its entrance point into the film (over 1 mm according to **Figure S1**). As apparent in **Figure 2A** of the main paper, the first fringes appear only about 0.5^0 below the critical angle and for these fringes the refractive index deviation between the actual optical path and that obtained under the assumption of a constant bulk index is less than 5×10^{-4}. The majority of the fringes is associated with incidence angles less than 1.0^0 below the critical angle, and then the refractive index deviation is less than 1×10^{-4}. It therefore seems justifiable to neglect the refractive index gradient for the films presented in the main paper and treat the index as a bulk property (see eqns (2) and (24) of the main paper). Of course, all these considerations are only important in the presence of a refractive index gradient. Once the uptake process has reached equilibrium and the refractive index is uniform throughout the film the refractive index measurements have a precision of 3×10^{-5} as described in section 4.1 of the main text.

The displacement of the ray from the point of entry creates a dark band in the images that help us to identify the critical angle. The dark band is expected to be a universal phenomenon but its

width depends on the optical configuration. For example a thick film will give a wider band compared to a thinner film. A tight focus on the film-substrate interface is also expected to give a broader band. The refractive index plays a rather subtle role, changing both the critical angle and the displacement distance. This phenomenon was not studied in great detail in this work.

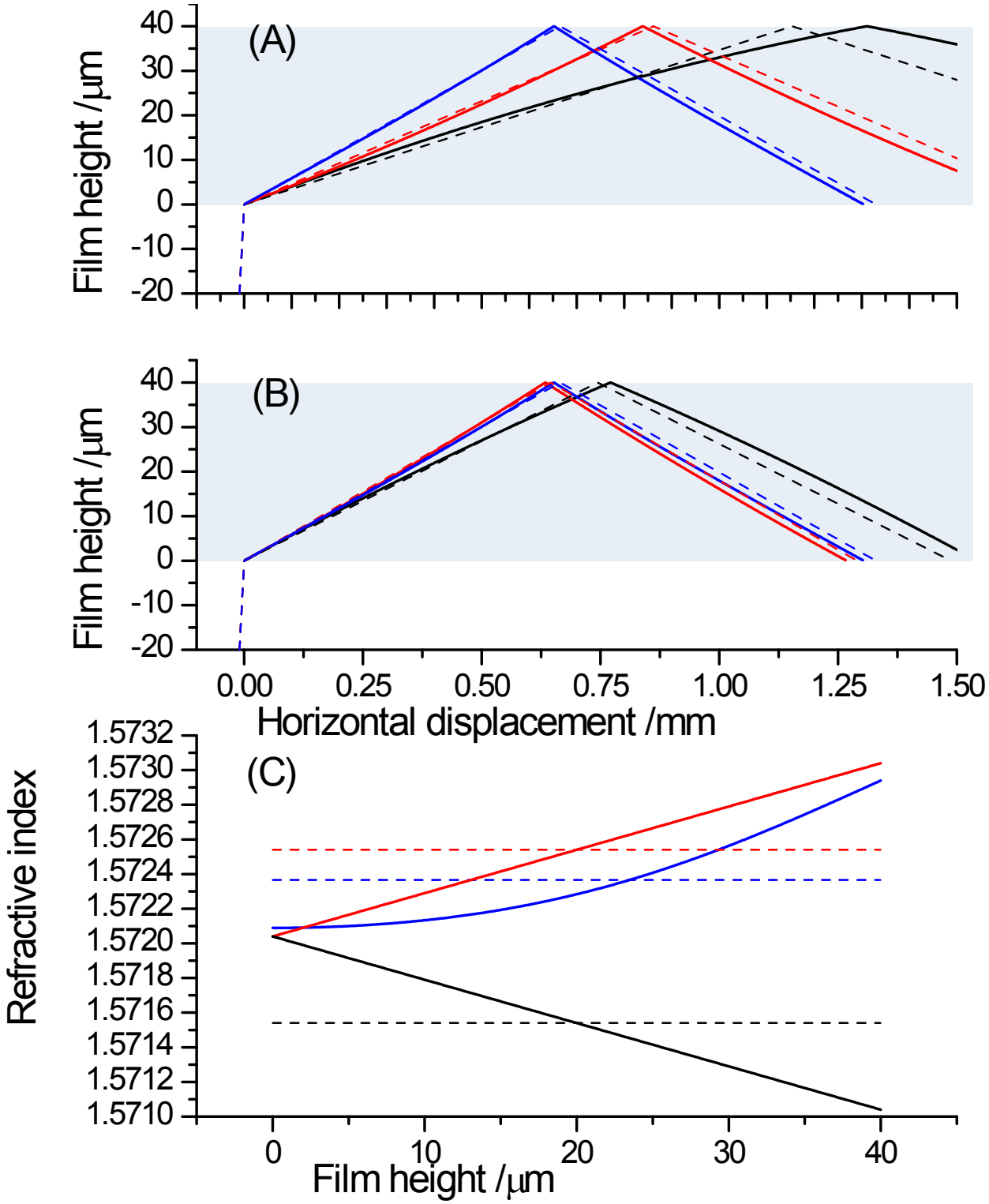

Figure S1: (A) Ray diagrams for different refractive index gradients calculated for an incidence angle of 64.28^0 and (B) 64.18^0 assuming a critical angle of 64.38^0. – Note the different length scale on the two axes. (C) Refractive index gradients assumed for panels (A) and (B). The blue curved line is calculated from the diffusion coefficient after a 100s time interval. The dashed lines are average refractive indices.

Section 2. Solubility parameters

In the main text the uptake of several solvents in SU-8 photoresist is discussed. Although the emphasis of the text was on the theoretical and experimental model, it is worthwhile to attempt a semiquantitative ranking of the different solvents' affinity to SU-8. Using solubility parameters of solvents and polymers it is possible to rationalize the interactions between sorbates and polymers. The Hildebrand solubility parameter for a liquid is defines as [1]

$$\delta = \sqrt{U / V_m} \qquad \text{* MERGEFORMAT (S7)}$$

where U is the cohesive energy, i.e. the energy required to vaporize a liquid into isolated molecules, and V_m is the molar volume of the liquid. At temperatures far below the liquid's boiling point the vaporization enthalpy of solvent may instead be used as an approximation: [1]

$$\delta = \sqrt{\frac{\Delta H_{vap} - RT}{V_m}} \qquad \text{* MERGEFORMAT (S8)}$$

Solvents with similar solubility parameters are expected to interact strongly and have the greatest mutual solubility, while those with very different values are immiscible. Also, solvents with comparable solubility parameters are expected to exhibit similar affinities behavior towards polymer materials. The cohesion parameter is analogous to the solubility parameter and used to describe non-liquids.[2] Optimal solubility of a polymer in a solvent is expected when the cohesion parameter of the polymer is close to the solubility parameter of the solvent. When the two parameters are mismatched, one may expect more or less pronounced swelling of the polymer.

More refined approaches, such as those of Hansen, distinguish the different intermolecular contributions to the solubility and cohesion parameters such as dispersion, polar (electrostatic), and hydrogen-bonding contributions.[3]

$$\delta^2 = \delta_D{}^2 + \delta_P{}^2 + \delta_H{}^2 \qquad \text{* MERGEFORMAT (S9)}$$

The interaction strength between a given solvent (1) and polymer (2) can be described using the distance between the solvent solubility coordinates and the centre of the polymers' cohesion sphere [3]

$$R_a = \sqrt{4\left(\delta_{D2} - \delta_{D1}\right)^2 + \left(\delta_{P2} - \delta_{P1}\right)^2 + \left(\delta_{H2} - \delta_{H1}\right)^2} \text{* MERGEFORMAT (S10)}$$

The closer the three solvent parameters are to the centre of the polymers solubility sphere the larger is the affinity of the polymer to this solvent. One can now define an interaction radius, $R_{0,}$ of the polymer at which the solvents show only marginal interactions with the polymer. It represents the boundary between solvents that will dissolve a polymer material and those that will have no interaction, i.e. only when $R_a / R_0 < 1$ a polymer is expected to be soluble in the given solvent. [3] Tables of solubility parameters are readily available in the literature for most common organic solvents and for many polymers. [2, 4] Hansen solubility parameters for some common organic solvents are listed in **Table S1** to support the discussion of the solvent interactions with SU-8.[4]

Table S1: Hansen Solubility Parameters for selected organic solvents. Solvents are sorted based on similar functionality. The three Hansen parameters are given in units of root pressure and the molar volumes are given in units of L/mol.[2, 4]

Index	Solvent	δ_D ($MPa^{1/2}$)	δ_P ($MPa^{1/2}$)	δ_H ($MPa^{1/2}$)	V_m ($Lmol^{-1}$)
1	n-Butane	14.1	0.0	0.0	101.4
2	n-Pentane	14.5	0.0	0.0	116.2
3	n-Hexane	14.9	0.0	0.0	131.6
4	n-Heptane	15.3	0.0	0.0	147.4
5	n-Octane	15.5	0.0	0.0	163.5
6	n-Decane	15.7	0.0	0.0	195.9
7	Cyclopentane	16.4	0.0	1.8	94.9
8	Cyclohexane	16.8	0.0	0.2	108.7
9	Benzene	18.4	0.0	2.0	89.4
10	Toluene	18.0	1.4	2.0	106.8
11	Ethylbenzene	17.8	0.6	1.4	123.1
12	o-Xylene	17.8	1.0	3.1	121.2
13	p-Xylene	17.6	1.0	3.1	123.3
14	Naphthalene	19.2	2.0	5.9	111.5
15	Chlorobenzene	19.0	4.3	2.0	102.1
16	Aniline	19.4	5.1	10.2	91.5
17	Benzaldehyde	19.4	7.4	5.3	101.5
18	Phenol	18.0	5.9	14.9	87.5
19	Anisole	17.8	4.1	6.7	119.1
20	Bisphenol-A	19.2	5.9	13.8	207.5
21	Chloromethane	15.3	6.1	3.9	55.4
22	Dichloromethane	18.2	6.3	6.1	63.9
23	Chloroform	17.8	3.1	5.7	80.7
24	Carbon Tetrachloride	17.8	0.0	0.6	97.1
25	Trichloroethylene	18.0	3.1	5.3	90.2
26	Methanol	15.1	12.3	22.3	40.7
27	Ethanol	15.8	8.8	19.4	58.5

28	1-Propanol	16.0	6.8	17.4	75.2
29	2-Propanol	15.8	6.1	16.4	76.8
30	1-Butanol	16.0	5.7	15.8	91.5
31	Tertbutyl Alcohol	15.2	5.1	14.7	95.8
32	Ethylene Glycol	17.0	11.0	26.0	55.8
33	Glycerol	17.4	12.1	29.3	73.3
34	Water	15.5	16.0	42.3	18.0
35	Dimethyl Ether	15.2	6.1	5.7	63.2
36	Diethyl Ether	14.5	2.9	5.1	104.8
37	Methylethyl Ether	14.7	4.9	6.2	84.1
38	Tetrahydrofuran	16.8	5.7	8.0	81.7
39	1,4 Dioxane	19.0	1.8	7.4	85.7
40	Ammonia	13.7	15.7	17.8	20.8
41	Methylamine	13.0	7.3	17.3	44.4
42	Ethylamine	15.0	5.6	10.7	65.6
43	Dimethylamine	15.3	4.8	11.2	66.2
44	Diethylamine	14.9	2.3	6.1	103.2
45	Ethylenediamine	16.6	8.8	17.0	67.3
46	Acetonitrile	15.3	18.0	6.1	52.6
47	Formaldehyde	12.8	14.4	15.4	36.8
48	Acetone	15.5	10.4	7.0	74.0
49	Acetic Acid	14.5	8.0	13.5	57.1
50	Acetylchloride	16.2	11.2	5.8	71.4
51	Ethylacetate	15.8	5.3	7.2	98.5
52	Acetic Anhydride	16.0	11.7	10.2	94.5
53	Acrylylchloride	16.2	11.6	5.4	81.3
54	Cyclopentanone	17.9	11.9	5.2	89.1
55	Gamma-butyrolactone	19.0	16.6	7.4	76.8
56	PGMEA*	15.6	5.6	9.8	137.1
57	Acetamide	17.3	18.7	22.4	60.8

58	N,N Dimethylformamide	17.4	13.7	11.3	77.0
59	N,N Dimethylacetamide	16.8	11.5	10.2	92.5
60	Dimethylsulfoxide	18.4	16.4	10.2	71.3

*PropyleneGlycol Monomethyl Ether Acetate

The cohesion parameters for many commercial polymers have also been determined.[2, 4] Unfortunately, we were not able to obtain solubility parameters for SU-8 photoresist. Typically, a comparison is therefore made to similar structured epoxies.[5] SU-8 is a glycidyl ether of Bisphenol A Novolac and one may compare SU-8 therefore to either glycidyl ether of Bisphenol A resin, (such as many EPON and EPIKOTE resins) or to glycidyl ether of Novolacs such as the Dow Epoxy Novolac (DEN) resins. The structures of these materials are shown in **Scheme S1** [6, 7] and their cohesion parameters in **Table S2**.

Table S2: The cohesion parameters of polymers similar to SU-8. The three Hansen parameters for dispersion, polar and hydrogen bonding interactions are presented in units of root pressures. The interaction radius of each polymer, R_o, is also given.

Polymer	**δ_D (MPa$^{1/2}$)**	**δ_P (MPa$^{1/2}$)**	**δ_H (MPa$^{1/2}$)**	**R_0 (MPa$^{1/2}$)**
EPON 1001	17.0	9.6	7.8	7.1
EPIKOTE 1001	20.00	10.32	10.11	10.02
EPIKOTE 1001 (10%)	18.1	11.4	9.0	9.1
EPIKOTE 1004	17.4	10.5	9.0	7.9
DEN 438	20.3	15.4	5.3	15.1
DEN 444	19.5	11.6	9.3	10.0

Scheme S1: *The structure of several common epoxy precursor units, glycidyl ether of Novolac (DEN 438 and DEN 444), glycidyl ether of Bisphenol A (EPON 1001, EPIKOTE 1001 and EPIKOTE 1004), and glycidyl ether of Bisphenol A Novolac tetramer unit (SU-8), are shown.*[6, 7]

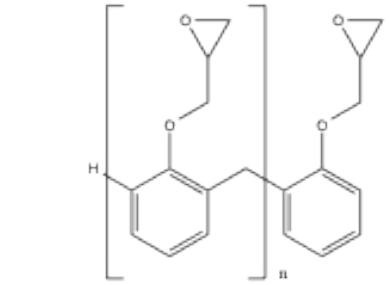

Glycidylether of Novolac
(DEN 438, DEN 444)

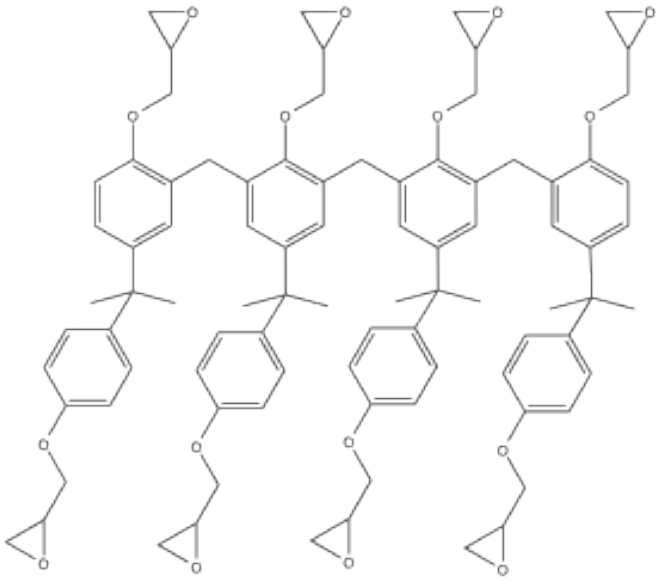

Glycidyether of Bisphenol A Novolac
(SU-8)

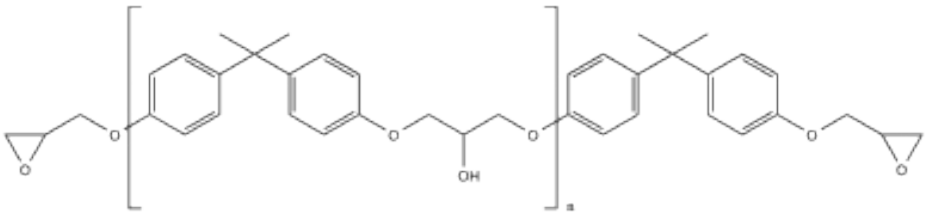

Glycidylether of Bisphenol A
(EPON 1001, EPIKOTE 1001, EPIKOTE 1004)

While the structures in Scheme S1 appear similar to SU-8 the degree of crosslinking is much higher in SU-8 compared with the other epoxy resins. This should offer SU-8 enhanced chemical resistance and a smaller interaction radius compared to other epoxies.

To relate the solubility parameters of the solvents to those of the epoxy polymers, the interaction spheres of three representative polymers with small interaction radii (EPON 1001, EPIKOTE 1004 and DEN 444) are shown in **Figures S2 and S3**.

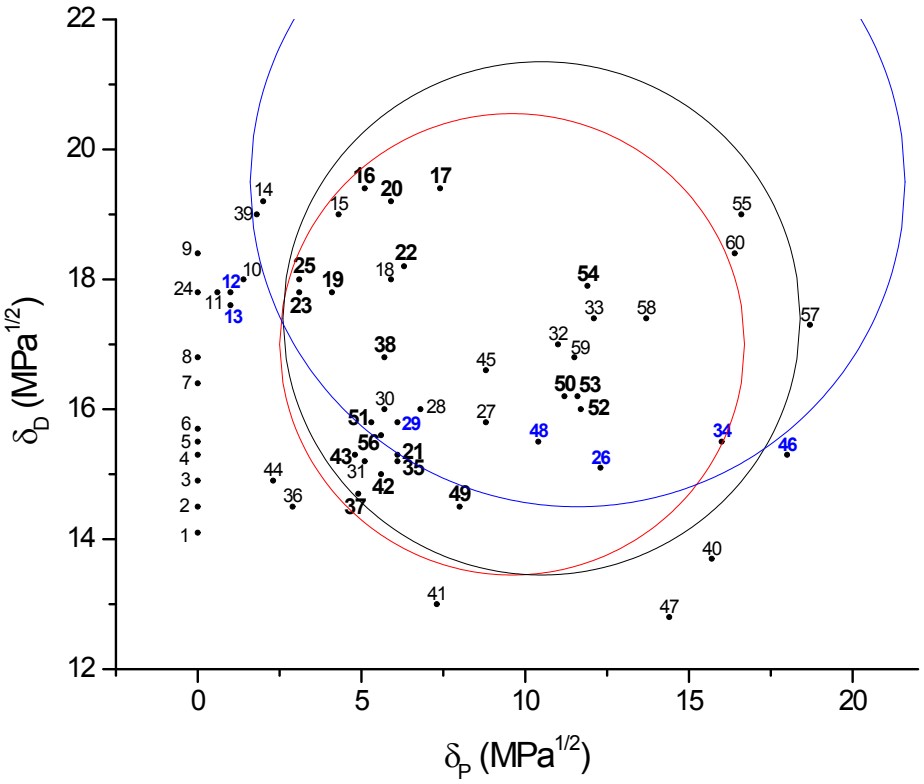

Figure S2: Hansen Solubility of 60 common organic solvents in the plane of dispersion and polar forces compared with the interaction radii of three different epoxies. The bold numbers indicate solvents that are within the solubility radii of EPON 1001 in both the Dispersion/Polar (shown here) and Hydrogen bonding/Polar planes (not shown). The indices in blue indicate solvents that were exposed to SU-8 in this study. The red circle, black circle and blue circle are the interaction radii of EPON 1001, EPIKOTE 1004 and DEN 444 respectively.

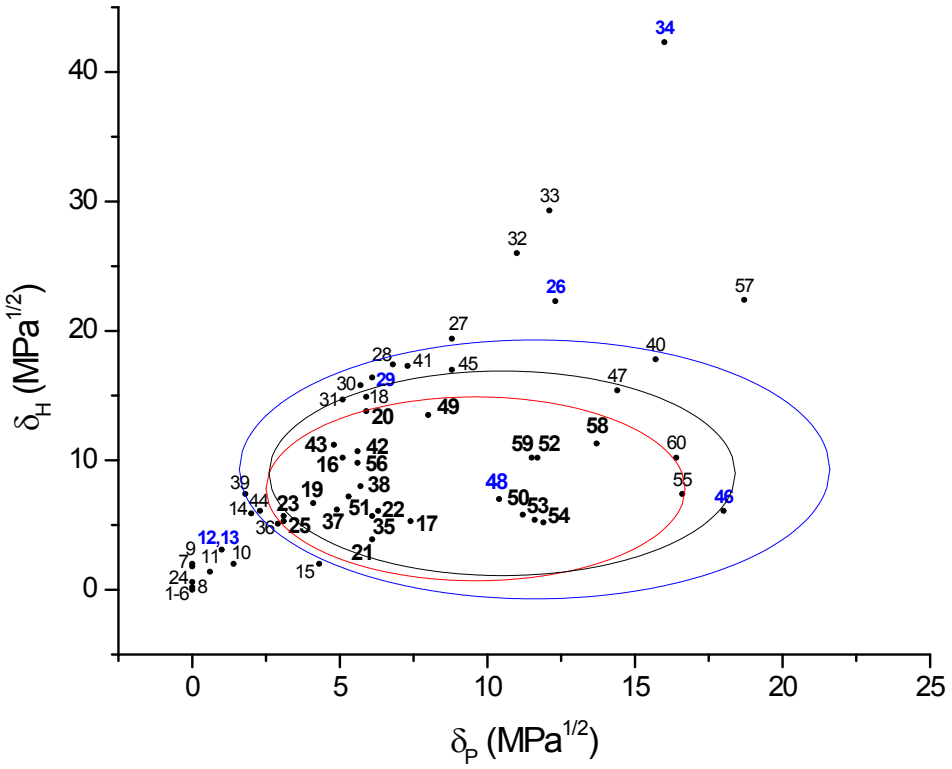

Figure S3: Hansen Solubility of 60 common organic solvents in the hydrogen bonding and polar forces plane compared with the interaction radii of three types of epoxies. The bold numbers indicate solvents that are within the solubility radii 1001 in both the Dispersion/Polar (not shown) and Hydrogen bonding/Polar planes (shown here). The indices in blue indicate solvents that were exposed to SU-8 in this study. The red circle, black circle and blue circle are the interaction radii of EPON 1001, EPIKOTE 1004 and DEN 444 respectively.

For example, in both Figures S2 and S3, the solvents we expect to interact with EPON 1001 are many chlorinated hydrocarbons, a series of ethers, amines, ketones and carboxylic acids. Gamma-butyrolactone (55) is the solvent used with SU-8 resists and is found close to the interaction boundary in Figures S2 and S3. Cyclopenatone is the solvent for SU-8 2000 series (54) and PGMEA is the developer used during SU-8 processing (56). Both were found within the solubility limits of EPON 1001.

By comparison in our experiments SU-8 films were exposed to several solvents and the interaction was monitored qualitatively. The relative interaction strength, R_a/R_0, was calculated from the above Hansen solubility parameters of EPON 1001 (Table S3). It is apparent that the Hansen model is not able to reproduce the strong interaction of SU-8 with methanol (and the weaker interactions with water) while predicting stronger than observed – and comparable interactions - of the epoxy with 2-propanol and xylene.

Table S3: Observed interactions of SU-8 to several solvents. For methanol, acetone and acetonitrile the films swelled rapidly and was delaminated after a few minutes. Swelling was observed for water and isopropanol. No swelling or any other effect was observed for exposure to m-xylene. The interaction strength R_a/R_0 is given for each solvent-epoxy pair. Values of $R_a/R_0 < 1$ indicate strong interactions and predict high mutual solubility.

Index	Solvent	SU-8 film response	R_a/R_0		
			EPON 1001	EPIKOTE 1004	DEN 444
48	Acetone	Dissolved	0.45	0.58	0.84
46	Acetonitrile	Dissolved	1.30	1.23	1.10
26	Methanol	Dissolved	2.14	1.92	1.57
34	Water	Swelling	4.96	4.59	3.42
29	2-Propanol	Minor Swelling	1.35	1.24	1.16
12/13	m-Xylene	No Swelling	1.39	1.51	1.29

The shortcomings of the Hansen solubility model are well known. The model fails to appropriately account for the influence of the solvent molar volume and the polymer's molecular weight.[4] This is especially problematic when working with high molecular weight polymers which are often less soluble than predicted. Additionally, polymers are often more soluble in solvents with small molar volumes ($V_m < 100$) than would otherwise be expected.[4]

Our experimental results agree with those by Ford who found that SU-8 was soluble in eight different solvents including acetone, acetonitrile, ethyl acetate, tetrahydrofuran and dioxane. This suggests that SU-8 also has an affinity to other small polar molecules containing carbonyl groups and ethers. It is then maybe not surprising to see a weak response to water and alcohols as well.

Of course, the solubility constants reported in the literature are specific to the preparation of the epoxies. The concentration of polymer in solution, and the solvent used at the time of casting can have significant effects on the degree of crosslinking in the material.[4] This could greatly change the physical behavior and solubility of a material. Additionally, solubility constants are temperature-dependent.[4] Moreover, since we could not obtain solubility parameters of SU-8 and we used values for similar epoxies that are presented in the literature as stand-ins. Considering all these limitations our experimental results agree well with the observation made by Ford et al. on the dissolution in acetone and acetonitrile.[5] The extension from dissolution in small ethers presented by Ford *et al.*[5] and in small alcohols in this study also seems plausible. The stronger than expected interactions of SU-8 with acetonitrile, methanol and water are likely due to the small molar volumes of these three solvents.

REFERENCES

1. A. F. M. Barton, *Chemical Reviews*, 1975, **75**, 731.
2. A. F. M. Barton, *CRC Handbook of Solubility Parameters and Other Cohesion Parameters*, CRC Press, Inc., Boca Raton, Florida USA, 2nd Edition edn., 1991.
3. C. Hansen, *Journal of Paint Technologies*, 1967, **39**, 104.
4. C. Hansen, M., *Hansen Solubility Parameters A User's Handbook*, CRC Press, Taylor & Francis Group, Boca Raton, Florida, USA, 2nd Edition edn., 2007.
5. J. Ford, S. R. Marder and S. Yang, *Chem. Mater.*, 2009, **21**, 476.
6. *Epoxy Resins: Chemistry and Technology*, Marcel Dekker, Inc., New York, New York, USA, Second edn., 1988.
7. *Physical Properties of Polymers Handbook*, Springer Science and Business Media, LLC, Second edn., 2007.